


REVIEW ARTICLE

Open Access



# Extreme index trends of daily gridded rainfall dataset (1960–2017) in Taiwan

Yu-Shiang Tung<sup>1\*</sup> , Chun-Yu Wang<sup>1</sup>, Shu-Ping Weng<sup>2</sup> and Chen-Dau Yang<sup>2</sup>

## Abstract

Previous lectures have shown that to effectively explore Taiwan's climate change or other relevant topics, long-term and stable observation datasets are required. We introduce the high-resolution gridded precipitation dataset (TCCIP\_PR), which was constructed by the Taiwan Climate Change projection and adaptation Information Platform (TCCIP) program from thousands of station records. Although, a high spatial-time relationship exists between the TCCIP\_PR and the stations, a large uncertainty occurs over the complex terrain on the southwest windward side during the summer, due to sparse stations. To better understand the change in the extreme rainfall trends, we analyze 9 suitable indices from the Expert Team on Climate Change Detection and Indices (ETCCDI). Our result show that the extreme rainfall intensity and frequency have continuously increased for a long time, and the consecutive dry days have decreased in recent decades, particularly over southwest Taiwan. The regime change evaluations agree that the precipitation characteristics were amplified and become more unpredictable from the early (1960–2002) to the late (2003–2017) period. For future applications or research, the calculated results of the extreme indices can be found in the printed documentation and the online retrieval system.

## Key Points

- High resolution grid rainfall data established by thousands of station records
- Extreme indices long-term trend detection
- Extreme rainfall regime change evaluation

**Keywords:** Climate change, Extreme index, TCCIP gridded dataset

## 1 Introduction

Due to the natural climate variability and industrial development in recent years, the emission of greenhouse gases has caused the global average temperature to rise. The scientific evidence has been very well presented and is mostly accepted by climate researchers. The positive effect on the precipitation changes has also been proved (Kharin et al. 2013). IPCC AR5 (Intergovernmental Panel

on Climate Change, Fifth Assessment Report) (Intergovernmental Panel on Climate Change 2014) showed that the global extreme rainfall events have generally increased over the past years. Many studies have also confirmed from the analysis of observations that the global average temperature rise will cause the frequency of extreme weather events to increase (Sillmann et al. 2013; Kharin et al. 2013; Liu et al. 2009). The global average temperature rise represents that the air moisture vapor content has increased, rendering the water vapor transfer to become strong. This extreme rainfall phenomenon will exhibit specific regional parameters for different large scale atmospheric systems, land-sea

\*Correspondence: [yushiangtom@gmail.com](mailto:yushiangtom@gmail.com)

<sup>1</sup> National Science and Technology Center for Disaster Reduction, 9F, No.200, Sec. 3, Beisin Rd., Xindian District, New Taipei City 23143, Taiwan  
Full list of author information is available at the end of the article

distribution, and topography. (Donat et al. 2013) introduced the extreme index ETCCDI (Expert Team on Climate Change Detection and Indices) by HadEX2 (Met Office Hadley Centre Global land-based gridded datasets of climate extremes indices version 2) to monitor the global climate extreme rainfall trend.

Taiwan has many unfavorable natural conditions, a complex topography, short and rapid rivers, and is also located in the East Asian monsoon region and north-west Pacific storm track. Moreover, Taiwan is affected by the frontal systems of the Mei-Yu Rain Season in May and June, and 3–4 typhoons hit the island annually (Wu and Kuo 1999; Central Weather Bureau). These extreme meteorological events can cause short-term and rapid heavy rainfall, resulting in flooding, landslides, slope collapse, etc. On the other hand, the southwest region of Taiwan during the dry season from September to April often experience many rainless days, which could cause droughts. As the extreme weather and climate in Taiwan may also be accompanied by natural disasters, the impact of the hydrological environment changes are important issues to understand. (Lu et al. 2012) used six daily weather station data to demonstrate the long-term trends of extreme indices, but it lacked the information regarding the dominated topographical regions. To satisfy the analysis, it would have been better if the reliable high spatial-time resolution grided dataset was used.

Starting from 1997, satellites have helped to collect high-resolution meteorological data related to the temperature, rainfall, radiation, etc. However, proving the argument that the trend in the data is related to climate changes requires long-term and stable station observed records. Previous studies of extreme climate literatures (Kharin et al. 2013; Donat et al. 2013; Sillmann et al. 2013; Endo et al. 2009) have focused on global or continental spatial scales, and the resolution has reached up to 50 or even 200 km. Even APHRODITE (Asian Precipitation—Highly-Resolved Observational Data Integration Towards Evaluation) (Yatagai et al. 2012) has provided the daily rainfall data in recent years covering a 25 km high-resolution over the Asian monsoon region. It is still difficult to show the small-regional based and high impact of extreme rainfall spatial distribution and intensity variation over Taiwan.

In addition to trying to understand the disasters accompanying Taiwan's extreme climate, we also study the geographical distribution characteristics and regime changes, which is conducive to conduct impact assessments and other application in different fields. Many studies used the dynamical and statistical downscaling with 5 km resolution grid data of Taiwan Climate Change projection and adaptation Information Platform (TCCIP) (Chen et al. 2016; Huang et al. 2016; Lee Yu-Chi

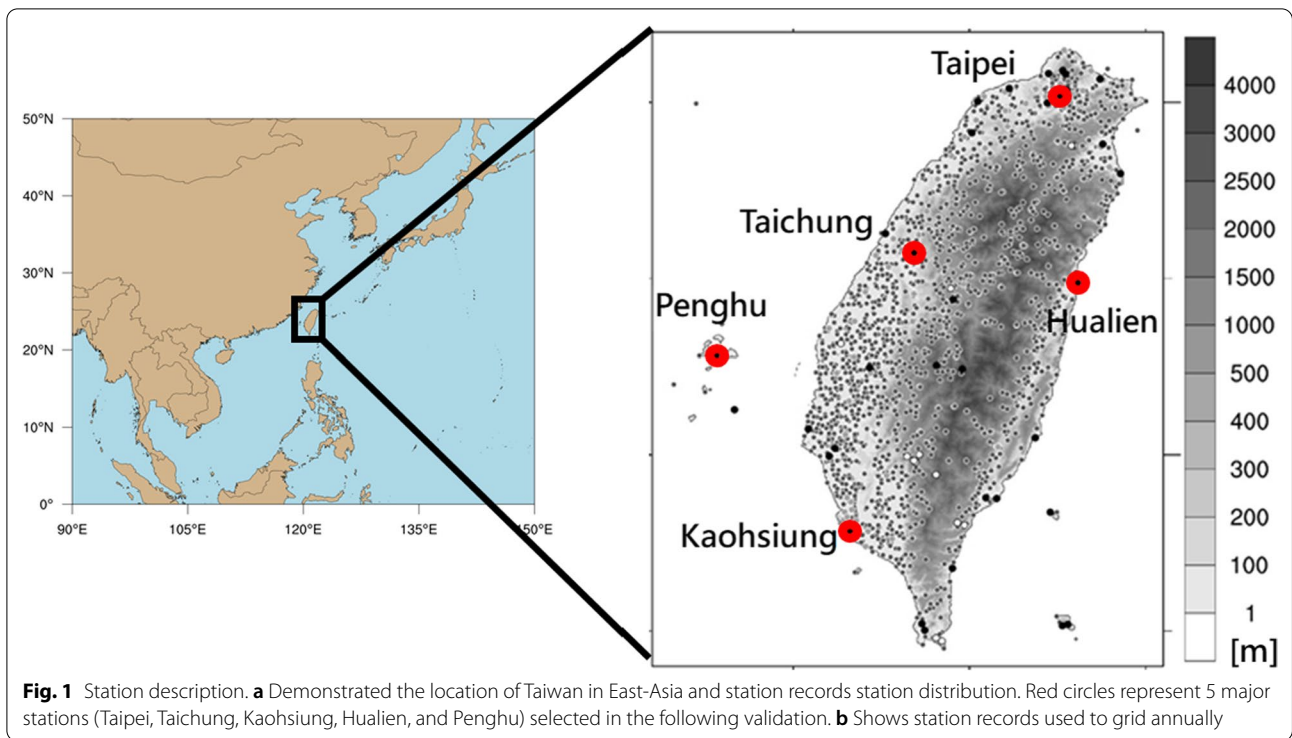
et al. 2019; Teng et al. 2021; Tung et al. 2016) for climate research, the evaluation of consistent regular observed dataset is worth for future reference. Considering the extreme rainfall trend, this study will make use of the station data and TCCIP gridded rainfall data to establish extreme indices database, and analyze its trend change. Sections 1 and 2 explain the source of the data and the analysis methods. Section 3 studies the results of the study, and Sect. 4 discusses the theory behind the results. The final section presents the conclusion of the study.

## 2 Data and methods

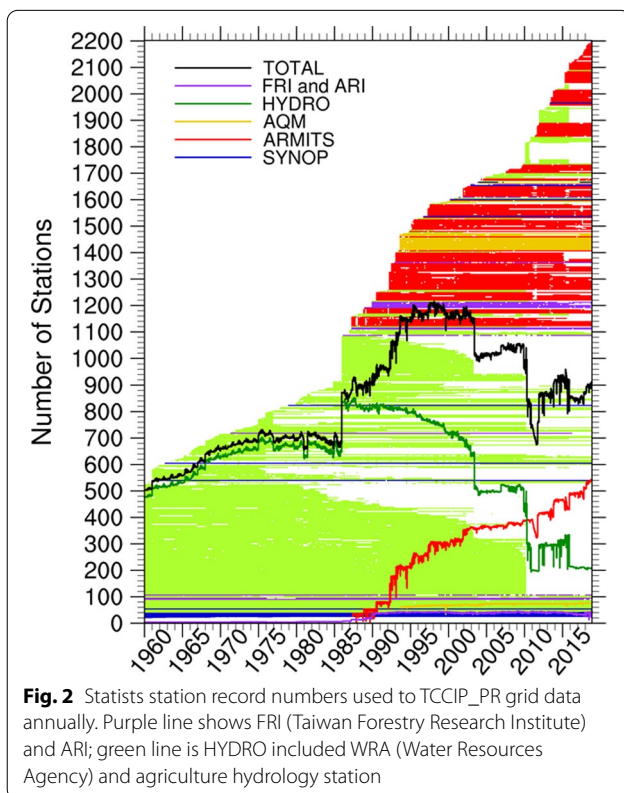
### 2.1 Data collection and gridding methodology

The establishment of ground observation stations in Taiwan stems from various requirements, such as disaster prevention, weather forecast, crop protection, etc. Many synoptic or automatic rainfall observation stations have been established in various places at different time points. TCCIP collects observational daily rainfall data from various units, digitizes the historical paper records, checks, filters, and homogenizes the data at the same time to obtain a reasonable digitization station dataset (Hung 2012). The dataset was updated regularly and extended to 2017. Since 1960, a total of 2203 stations have been set up throughout Taiwan, which contains CWB (Central Weather Bureau) and CAA (Civil Aeronautics Administration) synoptic stations (41 stations); automatic weather station (651 stations); WRA (Water Resources Agency) and agriculture hydrology stations (1337 stations); EPA (Environmental Protection Administration) air quality station (78 stations); TFRI (Taiwan Forestry Research Institute) stations (14 stations). The spatial location distribution can be found in Fig. 1.

However, the data quality of each station is unhomogenized, due to complex factors, such as funding maintenance and natural disasters. In addition, Fig. 2 shows that the complete and stable historical records are synoptic stations. Most of the older station records are hydrological stations that were set up for agriculture needs. After 1980, to better understand and forecast the weather, and thanks to the advancement of automatic observation techniques, CWB began to set up automatic stations to collect various atmospheric variables. To make up for the insufficient records covering the mountainous areas, the TFRI meteorological observation records that is used for ecological research was employed beginning from 2016. The raw data collected from the various sources were checked for the data integrity during the first stage. Before interpolating to the grids, the data was further checked for consistency and accuracy during the second stage. Even if only the station used a short-term record length in the background database, a regular 5 km resolution of the daily rainfall database (henceforth TCCIP\_PR)



could be established by the methodology of Weng and Yang (2018). TCCIP\_PR collected all QA (Quality Assurance)/QC (Quality Control) stations data and updated 1 km and 5 km resolution versions annually for variable requirements. We also chose 24 stable and long-term synoptic stations (Fig. 1 dark-black solid points) that was representative of Taiwan’s daily rainfall data to compare with the TCCIP\_RR to check the extreme index results. The red-colored points in Fig. 1 show five of the stations that were used to evaluate the extreme indices.



### 2.2 Extreme indices

The extreme indices (Sillmann et al. 2013) used in this study were developed by the ETCCDI experts who are under the WMO to analyze the long-term rainfall data can also be utilized to monitor and evaluate the global extreme climate changes. This paper focuses on the regional characteristics of rainfall extremes in Taiwan, and thus we select 9 indices for the long-term trends analysis. The definitions are described in Table 1. These indices are used to evaluate the precipitation and can be classified to intensity-based indices by RX1day, RX5day and SDII; total amount by R99pTOT, PrcpTOT; event type or relative to a fixed threshold value by RR1 and R80mm, which can be used to describe the extreme frequency events. Furthermore, the CWD and CDD can be used to describe the annually longest continuous events.

**Table 1** Extreme indices description

Index	Full name	definition
RX1day	Max 1-day precipitation amount	yearly maximum precipitation value of daily rainfall (mm)
RX5day	Max 5-day precipitation amount	The annual maximum accumulated precipitation for 5 consecutive days (mm)
R80mm	Heavy precipitation days	Daily precipitation value is greater than 80 mm This threshold definition comes from the disaster prevention application of CWB (day)
RR1	Rainy days	Daily precipitation above 1 mm ( $RR \geq 1$ mm) (day)
CDD	Consecutive dry days	Continuous accumulated daily precipitation less than 1 mm ( $RR < 1$ mm) (day)
CWD	Consecutive wet days	Continuous accumulated daily precipitation more than 1 mm ( $RR \geq 1$ mm) (day)
R99pTOT	Annual total Precipitation when $RR > 99p$	Cumulative total precipitation that RR reaches the 99th percentile threshold in period of 1961–1990. Where RR is daily precipitation above 1 mm (mm)
PrcpTOT	Annual total precipitation in wet days	Cumulative total precipitation of RR. Where RR is daily precipitation above 1 mm (mm)
SDII	Simple precipitation intensity index	Simple daily rainfall intensity, annual cumulative rainfall/rainy day (mm/day)

### 2.3 Evaluation methods

For the purpose to evaluate the annual extreme indices with large variance, (Taylor 2001) used statistical methods to evaluate the model performance. In this study, we set the station record data as the reference value to quantify the extreme indices analysis results of the grid data. The normalized root mean square error (NRMSE) is defined as

$$\text{NRMSE} = \frac{\text{RMSE}}{\sigma} \quad (1)$$

where *RMSE* is the index root mean square error of grids and stations, and  $\sigma$  is the standard deviation of the reference data (station record data).

The daily rainfall data from the station database underwent an imputation process when aligning to a grid. Still, the large fluctuation of the annual extreme indices affected the stability of the trend detection. Thus, during the trend evaluation of the extreme indices, to correctly evaluate the historical long-term change trend, the hydrological analysis common evaluation method of Theil-Sen (Yeh et al. 2016) was used. This method can calculate the reasonable linear trend and make the value less susceptible to outliers. Moreover, we also used the Mann–Kendall practices linear trend test to assume the data was a non-parametric and non-specific predetermined statistical distribution, and to test whether there were any significant trends (Yeh et al. 2016). Due to the large variance of the extreme index, the climate regime change evaluation used the U-Test (the Mann–Whitney-the Wilcoxon Test) (Pfeifer et al. 2015). This assumes the sample data is nonparametric when two climate periods are significantly different. According to the sorted data and the statistic scores level classification, the U value was less than 0.05, which can be viewed as passing the significant test.

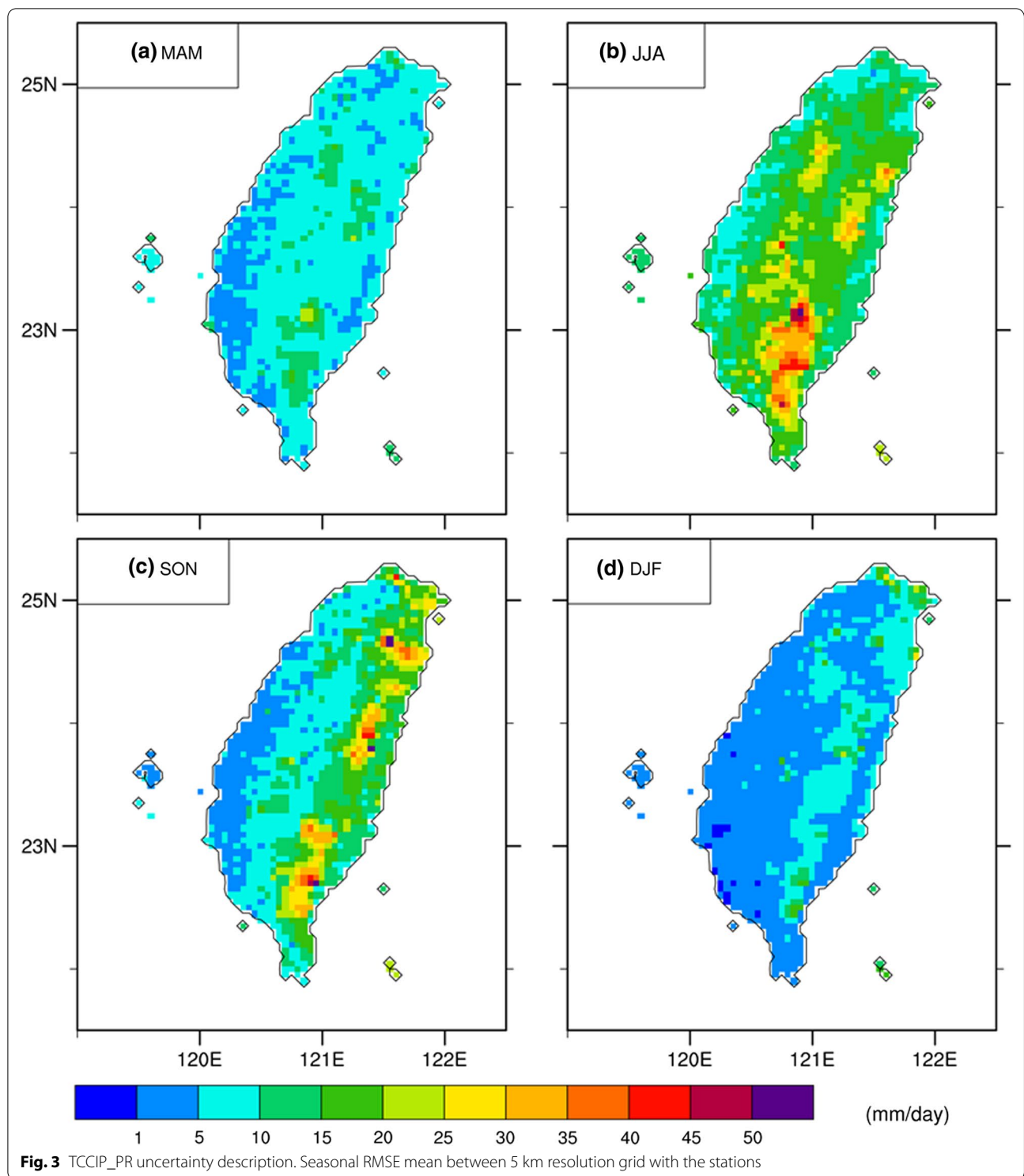
## 3 Results

### 3.1 Data evaluation and verification

Before applying TCCIP\_PR, we evaluated the uncertainty between the grid and the station data over the respective 5 km region. The article by Weng and Yang (2018) used rigorous methods and processes to conduct the evaluation. Errors could be generated during the data constructed process, which included the following: a. Optimized parameter algorithm, b. Station records imputation, and c. Distribution density of stations. The grid is representative of the entire coverage area, and may differ from the ground truth provided by the stations.

We used data that covered the 1960–2017 time period and evaluated the seasonal confidence between the station data and the recent grid, computing RMSE during the four respective seasons (spring MAM, summer JJA, autumn SON and winter DJF). In the wet season, the heavy rainfall is mostly contributed by typhoons, the southwesterly flow and other large-scale systems over the southwest windward side of mountainous areas. The errors in JJA will be 30–50 mm/day on average (Fig. 3b), and in SON presents a small region over the mountain area that exceeds 30 mm/day (Fig. 3c). By contrast, the small amount of rainfall during the dry season reveals fewer errors. The MAM rainfall patterns will only cause 15–20 mm/day errors over the mountainous area, and the DJF is not obvious (Fig. 3a, d).

Overall, the high distribution density and the stable quality of the station data over flat areas gives it a higher credibility than mountainous areas. Unfortunately, it is difficult to set up stations in mountainous areas due to logistics and funding reasons, thus causing the data quality to be less stable. Furthermore, the synoptic or small-scale systems (ex: summer afternoon convection) and extreme rainfall events (ex: southwest flow) that are windward to the mountains are likely to cause grid bias. Even so, it is worthy to note that compared to other



high-resolution rainfall grid data that have been commonly used in previous lectures (Tang et al. 2019; Thanh 2019; Yatagai et al. 2014), the grid data in this study is unique and provides many details. Though TCCIP\_PR

spans 5 km and 1 km versions and constructs by the same methodology, the slight difference was represented (Additional file 1: Fig. S1). The 5 km version spatial pattern of precipitation character consistent with 1 km

version. To evaluate the difference of time series, the monthly total precipitation is revealed the daily cumulated bias. Over the nearest grid point at Taipei station, the fluctuation is similar excepted the extreme precipitation contributed by typhoon events at the specific month (Additional file 1: Fig. S1b).

### 3.2 Extreme index

The rising trend of the average temperature can lead to changes in the extreme rainfall trend. Westra et al. (2013) applied 1960–2009 global ground station information and showed that a 1 deg.C global temperature rise would result in the maximum rainfall (the RX1day) to increase 7.2%. To understand the regional condition, the grid observation data can describe the climate and geographic distribution characteristics of the extreme indices in detail as opposed to the weather stations, which can only roughly describe the local environment. These two kinds of datasets provide different significance. By taking the rainfall intensity as an example, a single grid point value only describes the average condition of a 5 km grid area, while the position of the weather station represents the actual geographic location of the rainfall intensity. We used the grid observation data 1960–2017 as the historical base period to describe the spatial distribution of extreme indices, and split Taiwan into four geographic regions: North (NOR), Center (CEN), South (SOU) and East (EAS). We also used 24 stations to explain the extreme climate variability caused by global warming for the long-term trend analysis of Taiwan in recent years.

#### 3.2.1 Climatology

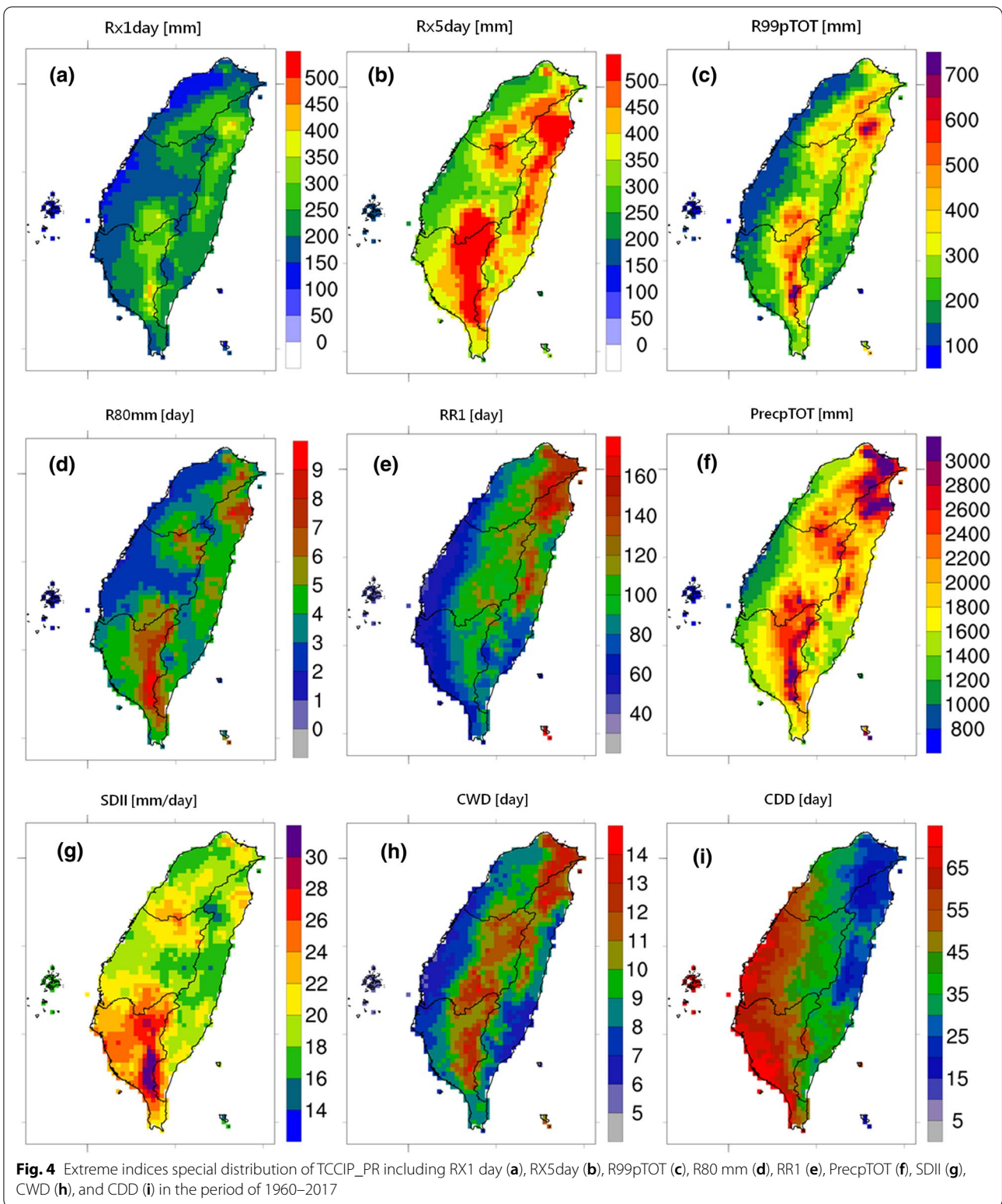
The annual maximum rainfall (RX1day) was distributed in the Yilan and Hualien mountainous areas, and is mainly affected by the northeasterly monsoon in the winter or the northwest track of typhoons. Meanwhile, the Kaohsiung and Pingtung mountainous areas is affected by the southwesterly stream in the summer. In addition, the topographic effect induced large precipitation was also likely to cause by the typhoon circulation (Fig. 4a). Even from the annual continuous 5 daily maximum cumulative rainfall (RX5day), similar climatic characteristics could be found (Fig. 4b), but the additional rainfall from the seasonal large-scale system needed to be sustained. The amount of precipitation was large enough to contribute to the RX5day. Specifically, the north, northeast, and eastern mountainous areas are vulnerable to the northeasterly monsoon on the windward side, and the southwest mountainous areas were contributed by the stream of the southwesterly monsoon and typhoon induced rainfall.

The extreme accumulated rainfall (R99pTOT) of the desired 99 percentile threshold rainfall, and the

reference ETCCDI (Sillmann et al. 2013) of WMO defined the 1961–1990 period as a historical reference climate. The computed rainy days (greater than or equal 1 [mm]) of the 99th percentile rainfall threshold and the yearly rainfall that exceeded the threshold were conducted via cumulative calculation. Thus, the R99pTOT will present nearly 30 years of contribution of the extreme rainfall (Fig. 4c). As for the definition of the current heavy rainfall event frequency, according to the Taiwan precipitation characteristics by the CWB, the daily rainfall was greater than 80 [mm] (R80mm) (Fig. 4d). The large value position of R80mm was similar to those occurred in RX1day, RX5day and R99pTOT in the northeastern. Over southwestern mountainous area, the R80mm is annually 8–9 days.

The following indices are often used in agriculture and water resources fields. The number of raining days (RR1) is defined as the daily rainfall  $\geq 1$  [mm] and is statistically calculated once in each year (Fig. 4e). More than 140 days (approximately 4.5 months) in north EAS Yilan every year is mainly due to the contribution of the northeasterly monsoon in the winter (Chen and Tu 2017; Hung and Kao 2010). Secondly, the typhoons in autumn or the ones that pass near Taiwan can also easily cause abundant rainfall due to the coupled effects (Chen 2011; Su et al. 2012; Wu and Kuo 1999). The southwest is a relatively dry region, excluding the time points when the summer monsoon accompanied by southwestern streams, afternoon convections, or typhoon circulation systems are present.

The total annual rainfall (PrctpTOT) is consistent with the RR1 (daily rainfall amount  $\geq 1$  [mm]) of the accumulated rainfall amount. Figure 4f shows that the annual reservoir inflow contributed by rainfall is most abundant over the northern region. The northern catchment area is on average contributed by the atmospheric rainfall at around 3000 [mm], Taoyuan catchment is 1800–2400 [mm] and the southern catchment area is 1800–2100 [mm] per year. The simple day rainfall intensity (SDII) (Fig. 4g) represents the PrctpTOT was equally distributed with the rainy days (RR1). The high-value area falls in the southwestern mountainous area at about 36 [mm/day], while the northeast area with the largest PrctpTOT is only 20 [mm/day] of SDII. The reason is that although the PrctpTOT in the southwestern region is more than the northeast area, the annual rainy day, compared with 4.5 months (130 days) above, represents the northern catchment rich water resource and the daily rainfall was evenly distributed (except some extreme weather events). By contrast, the PrctpTOT of the southwest mountain areas saw 3000 [mm], but the rainfall was concentrated at 1.5 months (80 days). This shows that the region tends to experience heavy



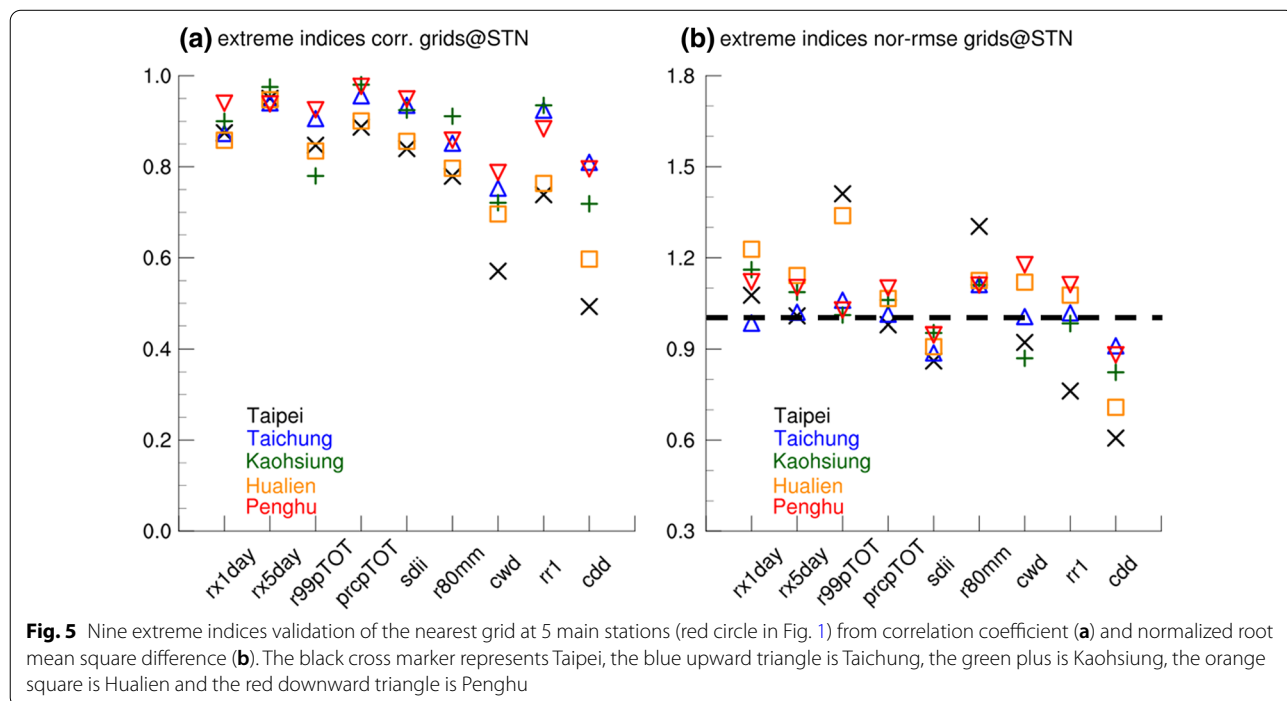
rainfall during short time patterns, rendering the water resource to be relatively unstable.

The index of consecutive wet days (CWD) where the daily precipitation required  $\geq 1$  [mm] was the calculated annual maximum. It represents the rain spell related to agriculture, which may affect the crop production. Figure 4h shows the northeastern region to be more associated with the large value and exhibiting an annual average of 12–14 days. Meanwhile, the main crop-producing areas of the western flat field were 6–7 days. When a large-scale system approaches, the southwest mountain area tends to rain for long consecutive days, due to the uplift of the terrain, ex: Mei-Yu front or southwesterly flow, etc. The definition of the longest consecutive dry day (CDD) (daily rainfall  $< 1$ [mm]), which could simply show the occurrence of meteorological drought, is opposite to that of CWD. Figure 4i shows the southwestern high and northeastern low. The west flat area from Taichung to Pingtung revealed consecutive 60 rainless days (approximately 2 months) per year at least.

Since the observation grid data and the station records have significant different characteristics, we will evaluate the data represented extreme indices. Figure 5 selects 5 representative stations in each area (the red dots in Fig. 1) and compare the time series correlation coefficients corresponding to the closest grid points (Fig. 5a). The normalized root mean square error (NRMSE) (Fig. 5b) shows data applied to the grid terminal of indices capacity assessment. While the

NRMSE value of the grid data is closer to 1, the deviation between the two is smaller.

The correlation coefficient of most indices at each station exceeds 0.7 and the NRMSE is less than 0.2, which reveals a high correlation and low bias. Because the grid value reveals a regional homogenized effect relative to the station data, the number of events obtained by the application calculation will mostly be different from the analysis results of the station, especially for the event type of extreme indices, which was calculated by threshold (R80mm, RR1, CDD, CWD), and the grid value was often lower than the position closest to the station. However, the spatial distribution and geographic characteristics tend to be consistent. Considering the varying technical performance for different regions, the correlation coefficient and NRMSE was close to 1 for the grid of Taichung and Penghu, due to a more homogeneous rainfall feature. As the grids of the TCCIP\_PR precipitation came from the rainfall gauges within the vicinity (Weng and Yang 2018), the more simple and consistent region resulted in a better relationship. By contrast, the precipitation of the Taipei grid, which was contributed by variable rainfall stations over a more complex topographic surrounding, revealed a weaker technical performance. This was similar to the Hualien grid. The seasonal RMSE mean evaluation between the grid and stations in the corresponding regions demonstrated consistent results (Fig. 3).





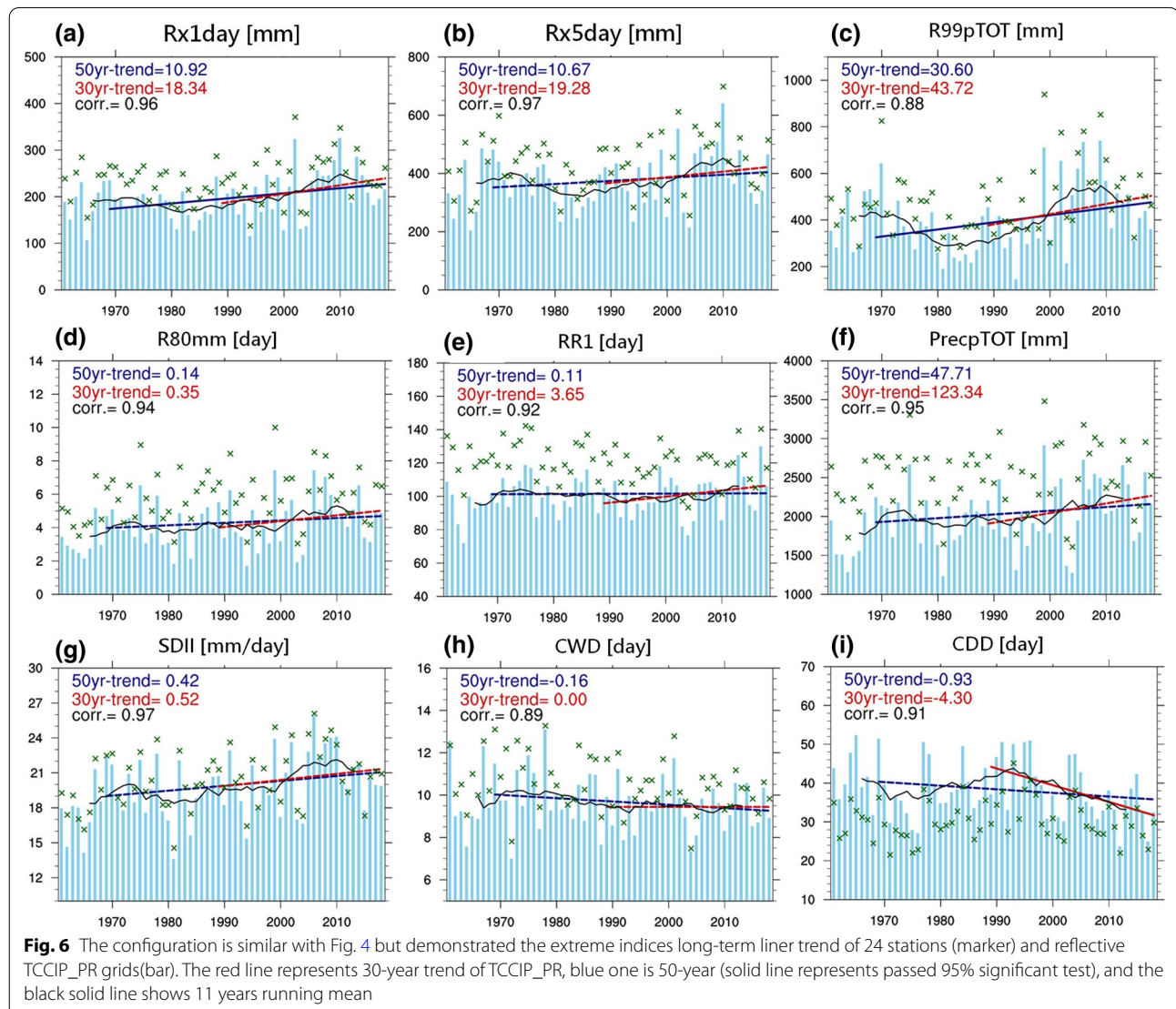
### 3.2.2 Long-term trend

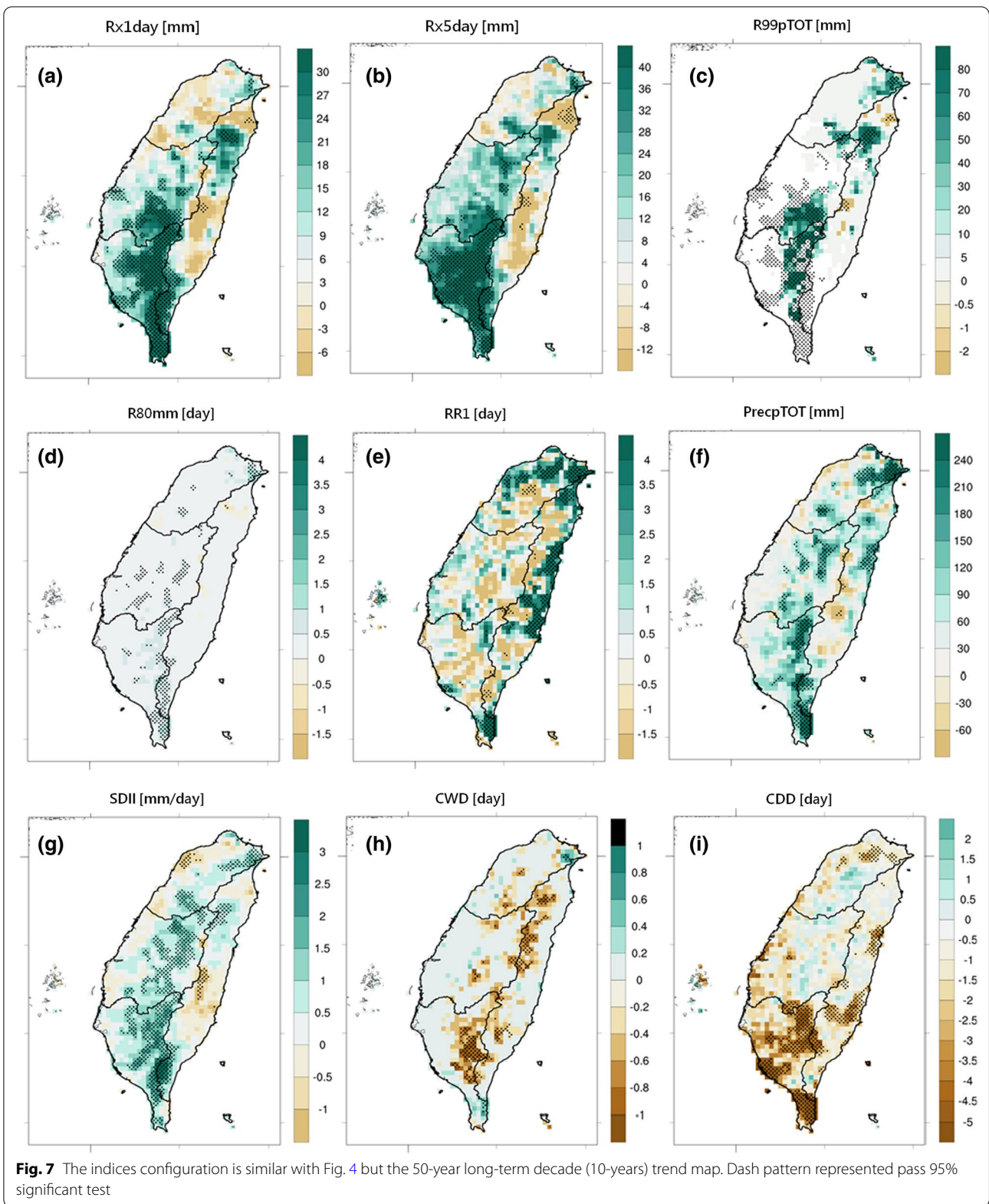
**3.2.2.1 Time series** To assess the long-term trend of extreme indices, the major analysis dataset of the TCCIP\_PR came from 24 stations, which was distributed throughout Taiwan (the location of the stations is denoted by the black filled dots in Fig. 1). This allowed the annual average of Taiwan to be calculated. Figure 6 shows the 1960–2017 extreme indices trends by the 30/50 years long-term linear trend and the 11 years running mean slowly fluctuating. The time series correlation coefficient of all the indices at the stations is significantly consistent (demonstrated at upper left legend of each plot). In the following paragraph, the trends are described in more detail.

The RX1day (Fig. 6a) 11-year running mean slowly rose, the 50-year trend presentation increased 10.92 [mm] per decade (pass significant test), and the 30-year trend increased more obviously. The RX5day 50-year and

30-year trend slowly rose (reject significant test) (Fig. 6b). The R99pTOT 11-year running mean revealed a decadal oscillation. The variation during the period of 1980–1990 was relatively low, while the 2000–2010 period was high and was decreasing in recent years. The trend of the 50-year was 30.6 [mm/Decade] (pass significant test). Figure 6d shows the R80mm 50/30-year linear trend slightly increased (reject significant test).

As the RX1day and RX5day are unable to distinguish between the seasons, the maximum value of whole year was used. Additionally, there was no direct relationship with the number and intensity of typhoons, resulting in only the climate change to be assessed. The heavy rainfall pattern increased significantly. R80mm did not change, but the R99pTOT showed an increasing trend, indicating that the intensity of a single extreme rainfall event increased. The aforementioned four indices associated





with the heavy rainfall (Fig. 7a–d) of the 11-year running mean showed that the situation significantly increased around 2000, which is similar with previous studies (Tung et al. 2016).

The SDII calculation involves a comprehensive index, where RR1 is divided by PrcpTOT. The annual value represents the daily precipitation distribution in Taiwan, and the long-term steady change of RR1 matches the slowly increasing trend of PrcpTOT. Furthermore, as mentioned previously, the grid and station data exhibit significantly different features. The indices of PrcpTOT and RR1 calculated by TCCIP\_PR are more underestimated when compared with the station data. However, SDII results from the precipitation ratio. As long as TCCIP\_PR of the PrcpTOT and RR1 own a stronger relationship with the annual variation of the station, SDII will be consistent with the trend of the station analysis results (Fig. 6g).

As the main contribution to the CWD annual variance is from the north/north-east (Fig. 4h), the continuous rainfall is dependent on the strength of the northeast monsoon and winter frontal systems. Previous lecture (Hung and Kao 2010) suggests the long-term downward trend of the precipitation reflects that the winter monsoon strength in East Asia significantly reduced after 1980. Although the CDD (Fig. 6i) 50-year trend declined (reject significant test), the 30-year trend significantly decreased (4.3[days/decade]) (pass significant test). The ETCCDI definition of CDD in an annual Julian day may underestimate the duration of the exact drought events during the dry season in Taiwan. The area average, which was above 40 days, indicated the extreme drought events could be attributed by the conditions of lacked precipitation during the spring time, even extended to Mei-Yu or typhoon season. This is a long-day phenomenon, which is not easy to rain (Cho and Lu 2013; Hung and Shih 2017; Weng and Yang 2018; Yang et al. 2019). Although the factors causing drought are considered complicated, CDD reflects the most basic risk factors of a meteorological drought.

TCCIP\_PR grid data shows a homogeneous regional precipitation. Some unexpected results appeared when comparing these two datasets, due to the generation of extreme indices. The TCCIP\_PR of the annual extreme precipitation indices of RX1day, RX5day, and R99pTOT will be underestimated. However, the large deviation of PrcpTOT comes from the accumulated daily precipitation bias. The key difference is if the grid and station data applied 1 [mm] as the index threshold value, there will be a systematic erroneous tendency of CDD overestimation. Since many dry days appear, but the precipitation can't attend to 1 [mm] threshold, the opposite index of RR1 becomes underestimated. This is despite the fact that the fluctuations and long-term trends are consistent.

**3.2.2.2 Spatial distribution** Figure 7 used the recent 50 years (1968–2017) daily rainfall data to analyze each extreme index decade trend. Considering the regions passed the significant test, the RX1day (Fig. 7a) and RX5day (Fig. 7b) had similar geographic distribution over the SOU areas, including Kaohsiung and Pingtung mountain area, where the rainfall respectively increased by 30 [mm] and 40 [mm]. The declining trend is mainly distributed in the north EAS flat region (Yilan) (6 and 12 [mm], pass significant test), EAS central region (Hualien and Taitung), as well as the NOR of the coastal areas (Taoyuan, Hsinchu and Miaoli) (reject significant test). R99pTOT (Fig. 7c) represents a weakly trend over the flat areas in the west, except CEN and SOU mountain regions (pass significant test), despite Fig. 3 suggesting a large uncertainty over this region. From the R80mm (Fig. 7d) perspective, Taiwan showed a slight increase (not to 1 [day]/decade).

RR1 (Fig. 7e) showed an increase of 4[day] in the NOR, EAS, and SOU coastal areas, but a decreasing trend in other areas. PrcpTOT (Fig. 7f) increased 210–240 [mm] in the NOR and sporadic decreased in the EAS mountainous area. According to the aforementioned analysis, the application of the comprehensive index of SDII on TCCIP\_PR has high credibility. Figure 7g shows an increasing trend in most of the mountain areas that are higher than 500 m in Taiwan. Over the SOU mountainous area, there was an increase of 3 [mm/day] (pass significant test), and a decrease of 1 [mm/day] in EAS mountainous areas and NOR coastal areas, respectively. The CWD (Fig. 7h) in most high mountains area showed a decreasing 0.8–1 [day] trend (pass significant test). The CDD (Fig. 7i) in the SOU region markedly reduce 5 [day], and the EAS region sporadically decrease 4 [day] (pass significant test).

### 3.2.3 Regime changes

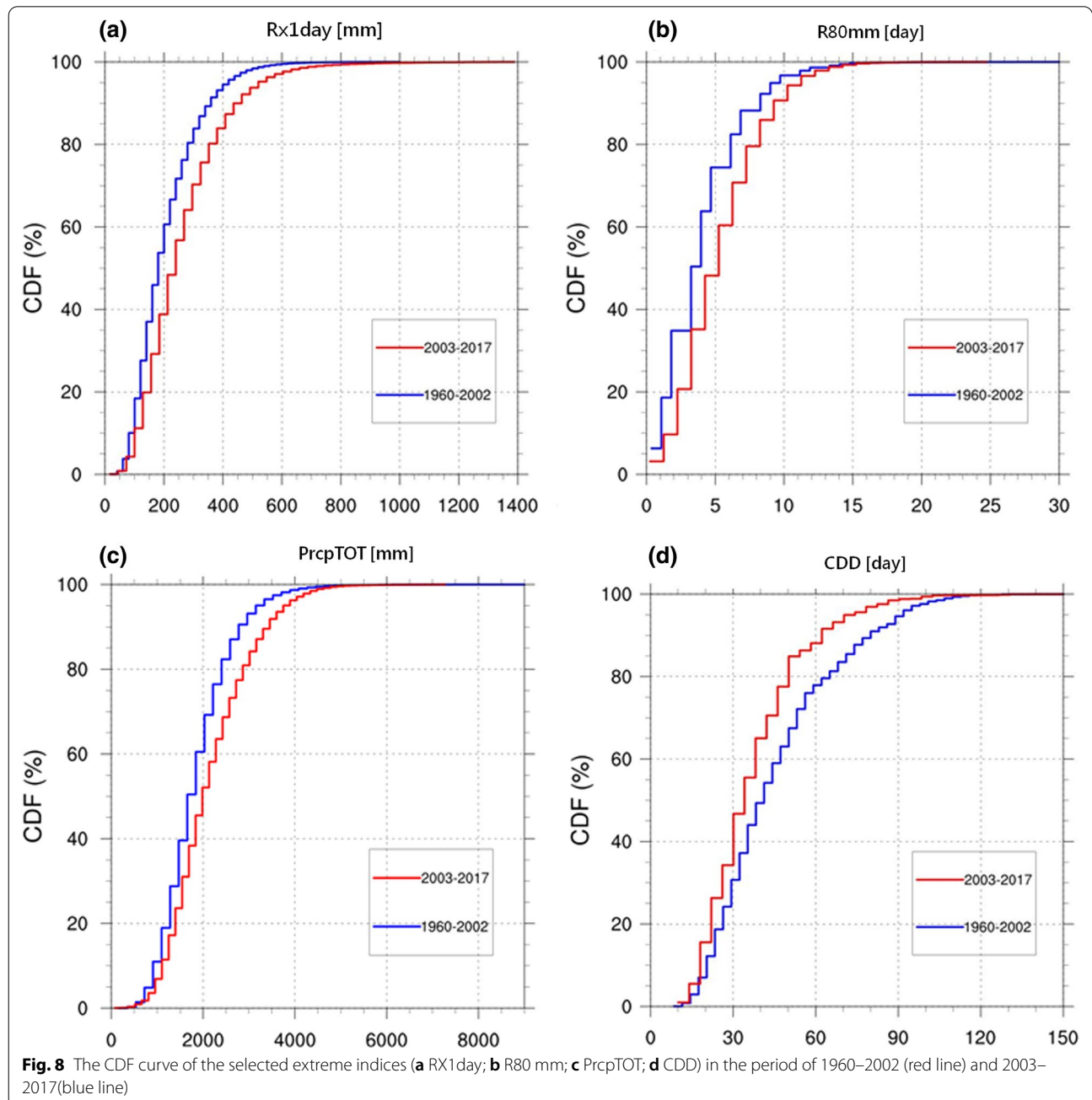
It is well known that the intensity, extension and variation of the western Pacific subtropical high (WPSH) affects the East Asian Summer monsoon rainfall and typhoon activity (Chen et al. 2010; Hung et al. 2020). Many lectures suggested the variation of WPSH had changed in the late 1990s (Huang et al. 2018, 2020). (Tung et al. 2016) pointed out the extreme rainfall long-term trends and mean state abruptly changed over Taiwan. Whether from the station or grid data, it was found that a “critical change point” in the extreme rainfall occurred in the 2002–2003 period. The climate pattern before and after the period differed notably. The intensity in the early period was relatively small, but increased more evidently in the later period.

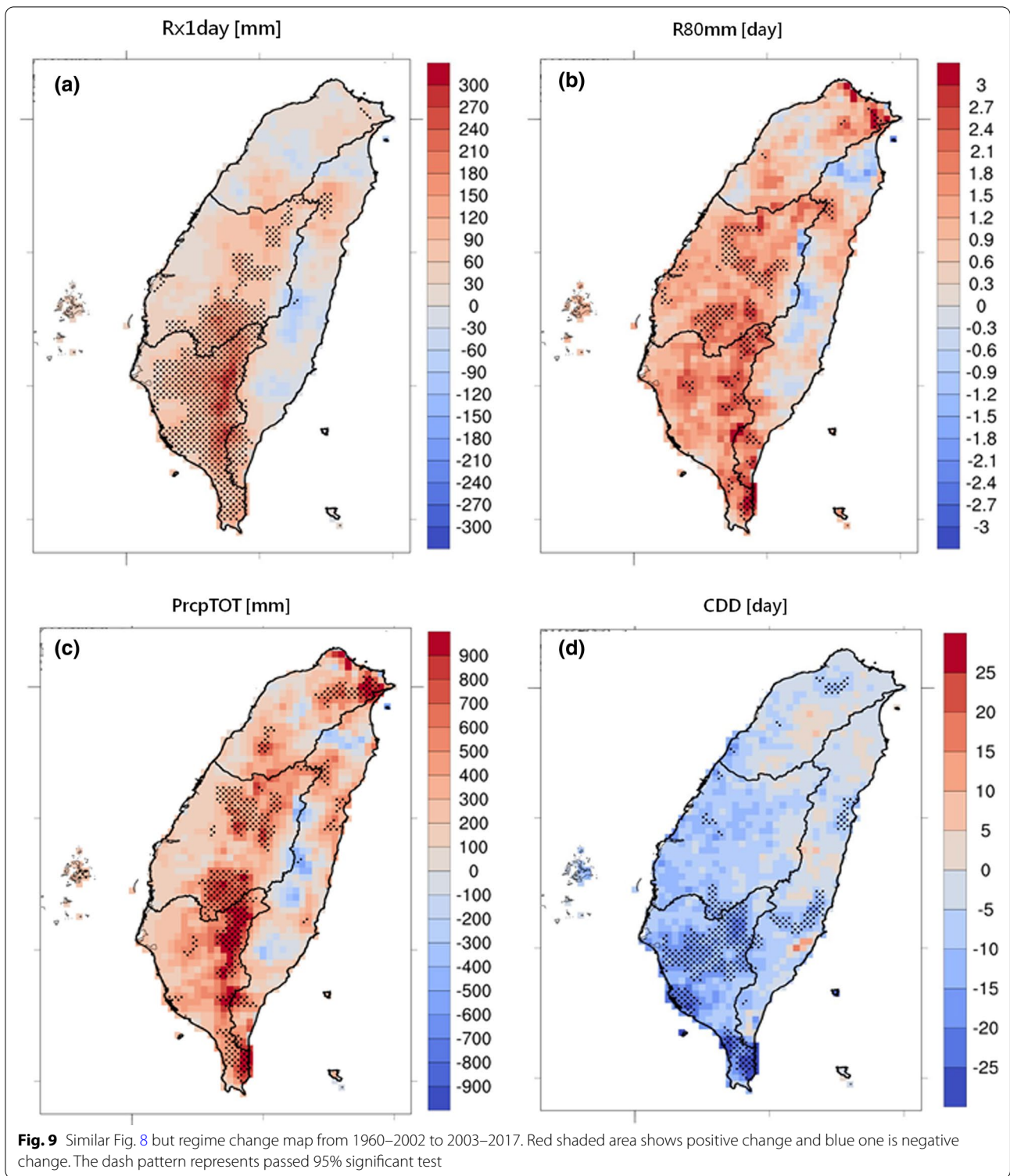
In order to understand the statistical distribution of the indices in the two periods, this study continued to

apply the relative analysis results to all the extreme indices and divides 1960–2002 (P1) and 2003–2017 (P2) two climatic periods. At the same time, each time step and grid was sample calculated cumulative distribution function (CDF). The following four indices with significant signals are selected for illustration (Fig. 8). The P2 of RX1day shows a shift to the right, however, the median (50 percentile) intensity from 170 [mm] (P1) increased to 230 [mm] (P2) (Fig. 8a). The median of R80mm from 4 [day] increased to 5.5 [day] (Fig. 8b); PrcpTOT from 1760

increased to 2000 [mm] (Fig. 8c). If the case of CDD is not considered, the P2 curve shifted to the left, and the median dropped from 41 to 34 [day] (Fig. 8d).

By looking at the changes in the spatial distribution, a different regional climate regime shift can be seen. Figure 9 shows the calculated extreme index difference from P1 to P2 (P2–P1) in each grid, along with the applied nonparametric statistics tests (U-test). The shaded areas show the statistically significant and climate variability analysis results. The RX1day in CEN and SOU showed a





higher increase in precipitation 30–60 [mm], and most of the SOU region may increase to 240 [mm] (pass significant test) (Fig. 9a). The R80 mm showed increased cases, and the CEN and SOU consistency increased 1–2 [day],

and the pass significant test mountainous areas added about 2–3 [day] (Fig. 9b). PrcpTOT also increased 800 [mm] or more over the mountainous areas (pass significant test) (Fig. 9c). On the CDD, most regions presented

reduced cases, and the SOU decreased 20 [day] or more (pass significant test) (Fig. 9d). From the long-term trend (Fig. 7), regime shift (Fig. 9) and spatial distribution of indices, it is found that the increase or reduction in the analysis results were consistent.

#### 4 Discussion

Due to the lack of historical long-term stable and dense observation station data in Taiwan, this paper tried to analyze the long-term historical changes in the past, which requires stable and accurate data sources for climate change research. In terms of the space density distribution over mountainous areas, the grid data limitation is more evident when compared to the inconsistent time length. Despite the effort to maximize the use of all possible records, using the 5 km resolution grid data to assess extreme rainfall still yields notable differences, because of the complex terrain. The same grid may cover both the windward and leeward side of the terrain, which shows obvious rainfall distribution differences. This introduces greater uncertainty to the mesh data that covers mountainous regions.

Prior to this, the studying of the natural variability of extreme rainfall indices will help provide evidence for future climate change research. Our analysis found that the RX1day, RX5day, R99pTOT exhibited strong changes and a linear upward trend. This is consistent with the literature (Henny et al. 2021). The change in the RX1day and RX5day spatial distribution trend showed that the area with the most obvious extreme rainfall increase was SOU. According to the trend analysis of SDII, the average rainfall intensity has also been increasing year by year.

In the wet season (from May to Oct.) of Taiwan, the extreme rainfall mainly comes from the Mei-Yu monsoon and typhoons. The Mei-Yu and summer southwest air streams are susceptible to the water vapor from the tropics/sub-tropics transport accompanied by strong rainfall. Another important rainfall contribution comes from typhoons, but the uncertainty in the path change is even more important. All these phenomena affect the horizontal position and intensity of WPSH. Hung et al. (2020) demonstrated the steering flow of WPSH dominated the typhoon tracks in the vicinity of Taiwan. Huang et al. (2020) presented the feature of WPSH began to change in the late 1990s by the ENSO event types. Tu et al. (2009) found that after the year 2000, the typhoon path of the Northwest Pacific followed a more northern trend, while the SOU was located at the windward side of the typhoon circulation. The airflow upwell, which was due to the terrain slope, also likely caused extreme rainfall.

In the dry season (from Sep. to Apr.), the climatology pattern of CDD (consecutive dry day) (Fig. 4i)

presented severe no-rainfall conditions over southwest Taiwan, which contributed a long-term decreasing trend (Fig. 6i). Kim and Kim (2020) suggested the EASM (East Asian Summer Monsoon) regional warming induced the rainband of the Mei-Yu front to shift southward to Taiwan in the early summer, which indicates that the dry season will withdraw earlier. Moreover, the atmosphere environment becomes more favourable to the diurnal convection, which cut-offs the CDD. Huang et al. (2019) used dynamic downscaling simulation data analysis under warming scenarios and indicated that the non-largescale weather system dominates the environmental airflow mechanisms.

To evaluate the evidence of the global climate regime change, long-term historical observations were used to describe the change frequencies, characteristics, and patterns of the average climate by rigorous inspection procedures (Lo and Hsu 2008). However, research (Allen et al. 2018) suggested that the climate trend of extreme rainfall has changed from a stable (or slight change) mode to a more variable (amplifying intensity and rainless) climate mode. Under the circumstances, it will take a longer time to revise (or no longer) the current climate that is prone to extreme weather patterns. This study indicates the climate regime shifted by RX1day, R80mm and PrcpTOT that tend to enhance the precipitation and amplify the intensity in the second epoch. Meanwhile, the CDD analysis reflected the annual dry season ended sooner. Although it is difficult to identify the actual cause of the extreme events atmospheric condition modes, the provision of the climate phenomenon information can be used for further research evidence.

Global warming leads to climate change, which has already been verified by the relevant literature provided by IPCC AR5 (Intergovernmental Panel on Climate Change 2014). Many studies (Li et al. 2019; Kusunoki and Arakawa 2012; Tung et al. 2020) suggest that the surface temperature rise enhances the east Asian summer monsoon circulation and precipitation. The temperature rise also leads to an increased evapotranspiration from the ocean, which is reflected in the circulation of water vapor. Conditions are more conducive for the occurrence of heavy rainfall driven by the large-scale severe weather systems. Compared with the pre-industrial revolution, the global average temperature has risen by 1 degree Celsius, and the atmosphere physical phenomena are also reflected in the rainfall (Allen et al. 2018). However, there is still no complete discussion and verification of the issues related to Taiwan's extreme rainfall changes and the contribution of anthropogenic greenhouse gas emissions.

## 5 Conclusion

The TCCIP\_PR data collection spanned from 1960 to 2017. A total of 2203 station ground truth data which was scattered throughout Taiwan, produced 5 km high-resolution grid rainfall information. At present, the establishment of a grid data set by such a high-density station network to monitor the changes of regional climate rainfall for a long time is unique and rare. Regardless of the timing or average climate variation, the position of the corresponding station grid points is with high consistency and confidence. However, the complex terrain area exhibits a lower density spatial distribution of stations. In the summer, as the southwest windward side is particularly associated with extreme rainfall, this also induces a large uncertainty in the grid data.

This study demonstrates the extreme rainfall characteristics and climatology seasonal patterns over Taiwan. The extreme rainfall hot spots are over the northeast and southwest windward side mountain areas (e.g., RX1day, RX5day, R99pTOT and R80mm). The water resources are distributed from the abundant northeast to the inadequate southwest (e.g., RR1, PrcpTOT, CWD and CDD). The homogeneous precipitation feature is at the northeast, but the heavy rainfall is at the southwest (e.g., SDII). The extreme rainfall indices of the 50-year long-term trend shows that the total rainfall (PrecpTOT) continued to increase, but the number of rainy days (RR1) did not change, which signals that the average rainfall intensity (SDII) slightly increased. The frequency of heavy precipitation days (R80mm) did not show an obvious change, but the intensity of the annual maximum precipitation (RX1day/RX5day) significantly increased, as reflected by the R99pTOT, especially in the southwest region. Although some of the factors that affect the number of consecutive dry days (CDD) has weakened in recent years, it is still worthy to conduct further research to fully understand the mechanisms.

The climate regime changes of extreme indices validation compared the early (1960–2002) and late (2003–2017) time periods. It was found that the extreme rainfall intensity (RX1day), frequency (R80mm) and total amount (PrcpTOT) showed a rising trend. Meanwhile, the number of consecutive dry days (CDD) exhibited a decreasing trend. In particular, the southwesterly flow regime change induced all the indices significant regime to shift to the windward side.

The nine indices used in this study provide reader credibility and the climate regime change evaluations have been statistically verified. These results can be obtained at an online data archive (<https://tccip.ncdr.nat.gov.tw/>). The TCCIP\_PR continues to be extended and updated.

## Supplementary Information

The online version contains supplementary material available at <https://doi.org/10.1007/s44195-022-00009-z>.

**Additional file 1.** The comparison of different resolutions of TCCIP\_PR.

### Acknowledgements

Comments from the Anonymous Reviewers are much appreciated. We are also appreciated CWB (Central Weather Bureau), CAA (Civil Aeronautics Administration), WRA (Water Resources Agency), EPA (Environmental Protection Administration), TFRI (Taiwan Forestry Research Institute) proved the station historical records. This paper is supported by Taiwan Climate Change projection and adaptation Information Platform (TCCIP) program (MOST 110-2621-M-865-001).

### Authors' contributions

All authors contributed to the study conception and design. Material preparation, data collection and analysis were performed by Yu-Shiang Tung, Chun-Yu Wang and Chen-Dau Yang. Methodology was performed by Shu-Ping Weng. The first draft of the manuscript was written by Yu-Shiang Tung and all authors commented on previous versions of the manuscript. All authors read and approved the final manuscript.

### Competing interests

The authors declare that they have no competing interests.

### Author details

<sup>1</sup>National Science and Technology Center for Disaster Reduction, 9F., No.200, Sec. 3, Beisin Rd., Xindian District, New Taipei City 23143, Taiwan. <sup>2</sup>Department of Geography, National Taiwan Normal University, Taipei, Taiwan.

Received: 29 January 2022 Accepted: 15 March 2022

Published online: 26 March 2022

### References

- Central Weather Bureau. FAQ for Typhoon. [https://www.cwb.gov.tw/V8/E/K/Encyclopedia/typhoon/index\\_all.html](https://www.cwb.gov.tw/V8/E/K/Encyclopedia/typhoon/index_all.html).
- Chen C-An (2011) The influence of typhoon tracks on Taiwan Precipitation. Master
- Chen H-F, Jien-Yi Tu (2017) The climatology and long-term changes of rainfall in Taiwan using TCCIP dataset. *Bull Geogr Soc China* 59:1–20. [https://doi.org/10.29972/BGSC.201712\\_\(59\).0001](https://doi.org/10.29972/BGSC.201712_(59).0001)
- Chen J-M, Li T, Shih C-F (2010) Tropical cyclone- and monsoon-induced rainfall variability in Taiwan. *J Clim* 23(15):4107–4120. <https://doi.org/10.1175/2010JCLI3355.1>
- Chen YJ, Chu JL, Tung CP, Yeh KC (2016) Climate change impacts on streamflow in Taiwan catchments based on statistical downscaling data. *Terr Atmos Ocean Sci* 27(5):741–755. <https://doi.org/10.3319/TAO.2016.07.20.01>
- Cho Y-M, Mong-Ming Lu (2013) An analysis of the extreme dry spells in Taiwan and its variations during the recent one hundred years. *Atmos Sci* 42(2):171–188
- Donat MG, Alexander LV, Yang H, Durre I, Vose R, Dunn RJH, Willett KM, Aguilar E, Brunet M, Caesar J, Hewitson B, Jack C, Klein Tank AMG, Kruger AC, Marengo J, Peterson TC, Renom M, Oria Rojas C, Rusticucci M, Salinger J, Elayah AS, Sekele SS, Srivastava AK, Trewin B, Villaruel C, Vincent LA, Zhai P, Zhang X, Kitching S (2013) Updated analyses of temperature and precipitation extreme indices since the beginning of the twentieth century: the HadEX2 dataset. *J Geophys Res Atmos* 118(5):2098–2118. <https://doi.org/10.1002/jgrd.50150>
- Endo N, Matsumoto J, Lwin T (2009) Trends in precipitation extremes over Southeast Asia. *SOLA* 5:168–171. <https://doi.org/10.2151/sola.2009-043>
- Henny L, Thorncroft CD, Hsu H-H, Bosart LF (2021) Extreme Rainfall in Taiwan: seasonal statistics and trends. *J Clim*. <https://doi.org/10.1175/JCLI-D-20-0999.1>
- Huang WR, Chang YH, Cheng CT, Hsu HH, Tu CY, Kitoh A (2016) Summer convective afternoon rainfall simulation and projection using WRF

- driven by global climate model. Part I: over Taiwan. *Terr Atmos Ocean Sci* 27(5):659–671. <https://doi.org/10.3319/TAO.2016.05.02.01>
- Huang Y, Wang B, Li X, Wang H (2018) Changes in the influence of the western Pacific subtropical high on Asian summer monsoon rainfall in the late 1990s. *Clim Dyn* 51(1–2):443–455. <https://doi.org/10.1007/s00382-017-3933-1>
- Huang W-R, Huang P-H, Chang Y-H, Cheng C-T, Hsu H-H, Tu C-Y, Kitoh A (2019) Dynamical downscaling simulation and future projection of extreme precipitation activities in Taiwan during the Mei-Yu seasons. *J Meteorol Soc Jpn Ser II* 97(2):481–499. <https://doi.org/10.2151/jmsj.2019-028>
- Huang Z, Zhang W, Geng X, Jin F-F (2020) Recent shift in the state of the western Pacific subtropical high due to ENSO change. *J Clim* 33(1):229–241. <https://doi.org/10.1175/JCLI-D-18-0873.1>
- Hung C-W (2012) The construction of TCCIP Taiwan rainfall index (TRI) and its applications. *J Geogr Sci* 67:73–96
- Hung C-W, Kao P-K (2010) Weakening of the winter monsoon and abrupt increase of winter rainfalls over northern Taiwan and Southern China in the early 1980s. *J Clim* 23(9):2357–2367. <https://doi.org/10.1175/2009JCLI3182.1>
- Hung C-W, Shih M-F (2017) Construction of the Taiwan meteorological drought index and the analysis of severe drought cases. *Atmos Sci* 45(2):145–166
- Hung C-W, Shih M-F, Lin T-Y (2020) The climatological analysis of typhoon tracks, steering flow, and the Pacific subtropical high in the vicinity of Taiwan and the Western North Pacific. *Atmosphere* 11(5):543. <https://doi.org/10.3390/atmos11050543>
- Intergovernmental Panel on Climate Change (2014) *Climate change 2013—the physical science basis*. Cambridge University Press, Cambridge
- Kharin VV, Zwiers FW, Zhang X, Wehner M (2013) Changes in temperature and precipitation extremes in the CMIP5 ensemble. *Clim Change* 119(2):345–357. <https://doi.org/10.1007/s10584-013-0705-8>
- Kim K-Y, Kim B-S (2020) The effect of regional warming on the East Asian summer monsoon. *Clim Dyn* 54(7–8):3259–3277. <https://doi.org/10.1007/s00382-020-05169-7>
- Kusunoki S, Arakawa O (2012) Change in the precipitation intensity of the East Asian summer monsoon projected by CMIP3 models. *Clim Dyn* 38(9–10):2055–2072. <https://doi.org/10.1007/s00382-011-1234-7>
- Li Z, Sun Y, Li T, Ding Y, Ting H (2019) Future changes in East Asian summer monsoon circulation and precipitation under 1.5 to 5 °C of warming. *Earth's Future* 7(12):1391–1406. <https://doi.org/10.1029/2019EF001276>
- Liu SC, Fu C, Shiu C-J, Chen J-P, Wu F (2009) Temperature dependence of global precipitation extremes. *Geophys Res Lett*. <https://doi.org/10.1029/2009GL040218>
- Lo T-T, Hsu H-H (2008) The early 1950s regime shift in temperature in Taiwan and East Asia. *Clim Dyn* 31(4):449–461. <https://doi.org/10.1007/s00382-007-0311-4>
- Lu M-M, Cho Y-M, Lee S-Y, Lee C-T, Lin Y-C (2012) Climate variations in Taiwan during 1911–2009. *Atmos Sci* 40(3):297–322
- Pfeifer S, Bülow K, Gobiet A, Häsler A, Mudelsee M, Otto J, Reich D, Teichmann C, Jacob D (2015) Robustness of ensemble climate projections analyzed with climate signal maps: seasonal and extreme precipitation for Germany. *Atmosphere* 6(5):677–698. <https://doi.org/10.3390/atmos6050677>
- Sillmann J, Kharin VV, Zhang X, Zwiers FW, Bronaugh D (2013) Climate extremes indices in the CMIP5 multimodel ensemble: part 1. Model evaluation in the present climate. *J Geophys Res Atmos* 118(4):1716–1733. <https://doi.org/10.1002/jgrd.50203>
- Su S-H, Kuo H-C, Hsu L-H, Yang Y-T (2012) Temporal and spatial characteristics of typhoon extreme rainfall in Taiwan. *J Meteorol Soc Jpn Ser II* 90(5):721–736. <https://doi.org/10.2151/jmsj.2012-510>
- Tang X, Zhang J, Wang G, Yang Q, Yang Y, Guan T, Liu C, Jin J, Liu Y, Bao Z (2019) Evaluating suitability of multiple precipitation products for the Lancang River Basin. *Chin Geogr Sci* 29(1):37–57. <https://doi.org/10.1007/s11769-019-1015-5>
- Taylor KE (2001) Summarizing multiple aspects of model performance in a single diagram. *J Geophys Res Atmos* 106(D7):7183–7192. <https://doi.org/10.1029/2000JD900719>
- Teng T-Y, Liu T-M, Tung Y-S, Cheng K-S (2021) Converting climate change gridded daily rainfall to station daily rainfall—a case study at Zengwen reservoir. *Water*. <https://doi.org/10.3390/w13111516>
- Thanh NT (2019) Evaluation of multi-precipitation products for multi-time scales and spatial distribution during 2007–2015. *Civil Eng J* 5(1):255. <https://doi.org/10.28991/cej-2019-03091242>
- Tu J-Y, Chou C, Chu P-S (2009) The abrupt shift of typhoon activity in the vicinity of Taiwan and its association with western North Pacific–East Asian climate change. *J Clim* 22(13):3617–3628. <https://doi.org/10.1175/2009JCLI2411.1>
- Tung Y-S, Chen C-T, Min S-K, Lin L-Y (2016a) Evaluating extreme rainfall changes over Taiwan using a standardized index. *Terr Atmos Ocean Sci* 27(5):705–715. <https://doi.org/10.3319/TAO.2016.06.13.03>
- Tung Y-S, Simon Wang S-Y, Chu J-L, Wu C-H, Chen Y-M, Cheng C-T, Lin L-Y (2020) Projected increase of the East Asian summer monsoon (Meiyu) in Taiwan by climate models with variable performance. *Meteorol Appl*. <https://doi.org/10.1002/met.1886>
- Weng S-P, Yang C-D (2012) The construction of monthly rainfall and temperature datasets with 1 km gridded resolution over Taiwan Area (1960–2009) and its application to climate projection in the near future (2015–2039). *Atmos Sci* 40(4):349–369
- Weng S-P, Yang C-D (2018) The construction and verification of daily gridded rainfall dataset (1960–2015) in Taiwan. *Taiwan Water Conservancy* 66(4):33–52
- Westra S, Alexander LV, Zwiers FW (2013) Global increasing trends in annual maximum daily precipitation. *J Clim* 26(11):3904–3918. <https://doi.org/10.1175/JCLI-D-12-00502.1>
- Wu C-C, Kuo Y-H (1999) Typhoons affecting Taiwan: current understanding and future challenges. *Bull Am Meteor Soc* 80(1):67–80. [https://doi.org/10.1175/1520-0477\(1999\)080%3c0067:TATCUA%3e2.0.CO;2](https://doi.org/10.1175/1520-0477(1999)080%3c0067:TATCUA%3e2.0.CO;2)
- Yang T-C, Chen J-M, Yu P-S, Kuo C-M, Tsai M-Y, Chen H (2019) Investigation of climatic teleconnection and predictability for spring rainfall in Taiwan. *J Taiwan Agric Eng*. [https://doi.org/10.29974/JTAE.20191265\(4\).0001](https://doi.org/10.29974/JTAE.20191265(4).0001)
- Yatagai A, Kamiguchi K, Arakawa O, Hamada A, Yasutomi N, Kitoh A (2012) APHRODITE: constructing a long-term daily gridded precipitation dataset for Asia based on a dense network of rain gauges. *Bull Am Meteor Soc* 93(9):1401–1415. <https://doi.org/10.1175/BAMS-D-11-00122.1>
- Yatagai A, Krishnamurti TN, Kumar V, Mishra AK, Simon A (2014) Use of APHRODITE Rain Gauge–Based Precipitation and TRMM 3B43 Products for Improving Asian Monsoon Seasonal Precipitation Forecasts by the Superensemble Method. *J Clim* 27(3):1062–1069. <https://doi.org/10.1175/JCLI-D-13-00332.1>
- Yeh C-F, Yeh H-F, Lee C-H (2016) Mann-Kendall test and Theil-Sen estimator for long-term spatial and temporal trends of streamflow in Taiwan. *J Chin Soil Water Conservat* 47:73–83
- Yu-Chi L, Chia-Chi W, Shu-Ping W, Cheng-Ta C, Chao-Tzuen C (2019) Future projections of meteorological drought characteristics in Taiwan. *Atmos Sci* 47(1):66–93. <https://doi.org/10.3966/025400022019034701003>

## Publisher's Note

Springer Nature remains neutral with regard to jurisdictional claims in published maps and institutional affiliations.

**Submit your manuscript to a SpringerOpen® journal and benefit from:**

- Convenient online submission
- Rigorous peer review
- Open access: articles freely available online
- High visibility within the field
- Retaining the copyright to your article

Submit your next manuscript at ► [springeropen.com](https://www.springeropen.com)